# Simplified State-Space Average Model and Control Strategy for the Dual Active Bridge Power Converter

Vrishabh Randive
*Dept. of Electrical Engineering, IIT Hyderabad*
Kandi 502285, India
ee19mtech01011@iith.ac.in

Rupesh Wandhare, *Member, IEEE*
*Dept. of Electrical Engineering, IIT Hyderabad*
Kandi 502285, India
rupesh@iith.ac.in

***Abstract*—This paper presents the simplified state-space average model of the Dual Active Bridge (DAB) power converter which eliminates the complexity in Fourier based model of the transformer excitation system. The proposed model has used for developing a current control and a multiple loop voltage control strategy for the bidirectional converter. The model derived in this paper can be easily used for the bi-directional converter topology employed in the application of fuel cell, electrical vehicle battery charging, solar water pumping projects, etc., where voltage ports with large voltage difference are encountered. Nowadays, in several power applications, bidirectional converters with galvanic isolation are in demand due to their lightweight and reasonable efficiency and a quick turnover of the design is desirable. The simplified model of DAB converter is used for compensator design and control strategy formulation. This model and analytically derived parameters are verified by simulations. All the relevant simulation results are provided in this paper to demonstrate the efficacy and validity of the proposed model for DAB converter. The presented work in this paper provides a guideline of close loop control design for several other applications of DAB power converter using its simplified model.**

***Index Terms*—Bidirectional power converter, Dual active bridge converter, High-frequency transformer, Phase shift control, State-space averaging.**

## I. Introduction

The DC-DC bidirectional converter are very popular for power exchange between energy storage such as battery, ultracapacitor, etc., and the DC port of inverters. This inverter may be standalone in nature feeding the isolated load, in case of autonomous systems or it may be grid-tied in nature exchanging energy with a power system. The voltage-source current-controlled half bridge converter is widely used for bi-directional power exchange between two voltage ports where voltage difference is less than 50% [1]. It is non-isolated topology and useful only in cases where galvanic isolation is not required. Further, the half bridge non-isolated topology suffers with poor efficiency in a case when voltage difference between ports is wide. Isolated version of DC-DC converters are extensively investigated for the conditions when power is transfered with high voltage transfer ratio and isolation is desired [2].

Several versions of high frequency power converters are available which can be used based on power level, source, and load conditions. Author Ravi *et. al.* [4] has provided the classification of the bidirectional dc-dc converter based on galvanic isolation. High frequency DC-DC bi-directional power converters based on full bridge voltage source converter are useful for the application with power level more than 1kW. It has the flexibility of choosing the direction of power flow as per our requirement as shown in Fig. 1. In the area of distributed energy generation with storage, the bidirectional converter is used for power and energy management between storage, source and load. This power converter is also exercised in microgrid and electric vehicle.

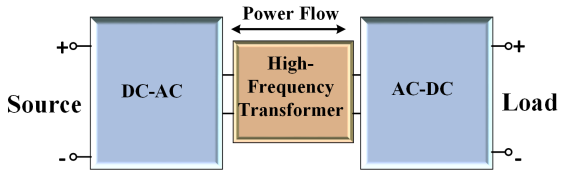


Fig. 1. Basic structure of Bidirectional Converter

This converter is operated for maintaining the power flow between two dc sources and load by applying proper switching and phase shifting between the gate pulses as shown in Fig. 1. A bi-directional converter with continuous inductor current and fixed switching frequency which impart zero voltage switching (ZVS) irrespective of the direction of power flow by using a simple auxiliary clamp circuit has demonstrated in [3]. Installation of renewable energy sources and storage interfacing the grid is monitored by the utility using stipulated standards formulated for the integration. Based on situation, the stake holder must ensure galvanic isolation between input port and the grid which may be followed on high-frequency transformer. The design consideration of high-frequency transformer is provided in [6].

This research work is supported by "Science and Engineering Research Board (SERB), Department of Science and Technology, Government of India", under the scheme Start-up Research Grant.

978-1-7281-6664-3/20/$31.00 ©2020 IEEE

The power generated from renewable energy sources are usually intermittent in nature and introduces additional complexity in the control. The modelling and analysis is needed for the implementation and design of the dc-dc converter. Authors Ardi *et al.* [5] have presented a detailed model and implemented the control of a non-isolated bidirectional DC-DC Converter with high voltage gain. Converter with a large number of devices increases the cost and size of the power conditioning unit. To overcome this problem, work presented in [9] demonstrated a system with less number of devices for the ZVS medium power bi-directional dc-dc converter.

In high frequency transformer based dc-dc bi-directional converter, for proper operation of the converter, phase shift should be adequately provided using phase shift control logic between the full-bridges at high and low voltage ports. It is observed that the converter behaviour varies from low frequency to high-frequency range. To explain the simplified analysis of phase shift controlled bi-directional converter, authors D. Xu *et al.* [7] assumed ideal switches and parasitic capacitors for reduction of switching losses. In several cases, the bidirectional converter consist of the voltage-fed converter at high voltage side and current-fed converter at low voltage side. The gross power transfer and its direction of flow is controlled by the phase-shifting angle between these two converters at both side of the high-frequency transformer. These converters utilize the leakage inductance of the high-frequency transformer as one of the element of the topology and it value is crucial in the converter design [8]- [10].

Authors H. Qin and J. W. Kimball [11] have presented a full order continuous time average model, in which dc terms and first-order harmonics are taken in the account via Fourier series expansion of the state variables. The DC term and the first-order harmonic of inductor current and capacitor voltage increases the complexity in the closed-loop design of the converter and results in to the third-order model.

This paper proposes the closed-loop current control approach for the DAB bi-directional converter by using simplified model of the converter. It reduces the complexity of traditional Fourier based model for DAB. The simplified model for this DAB converter ease in control design without deteriorating the control performance. The model further used for the voltage control using multiple loop. In this paper, section-II describes the operation of the converter with the switching states of both the bridges in forward and reverse direction of power flow. Section-III deals with the mathematical analysis of the converter followed by section-IV for the proposed simplified state-space average model. Further, this section provide the detail design of control strategy. The model is verified in section-V.

## II. Working of DAB Bi-directional Converter

The transformer primary voltage, $V_1$ and secondary voltage, $V_2$ relate with the power transfer between ports of the DAB power converter which is shown in Fig. 2, as follows [12]:

$$P = \frac{V_1 V_2}{n\ w_s L_{eq}} \theta \left(1 - \frac{\theta}{\pi}\right) \tag{1}$$

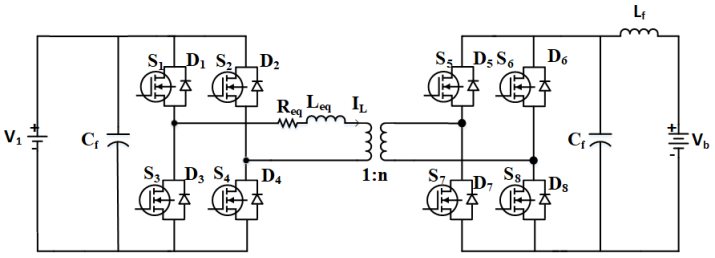


Fig. 2. Schematic diagram of single-phase DAB bidirectional converter.

where, $\theta$ is the phase angle difference between voltages $V_1$ and $V_2$, $w_s$ is the switching frequency of DAB is rad/sec, $L_{eq}$ is the equivalent inductor of the power converter, and $1:n$ is the transformation ratio of the transformer.

In this case, the high voltage port, $V_1$ can be DC link of hybrid system say photovoltaic terminals and DC link of the grid tied inverter (e.g. 400V). The low voltage port $V_2$ may be the energy storage: battery or ultracapacitor (48V).

### A. Buck operation (Forward power transfer)

In buck operating mode, the power transfers from high voltage port $V_1$ to the low voltage port $V_2$. In this mode, generated gate pulses of the HV side leads the LV side by an angle $\theta$ and power transfers from primary to secondary. Fig. 3 is showing the switching period of both bridges and current and voltage waveforms of the equivalent inductor. Table-I shows switching states of devices.

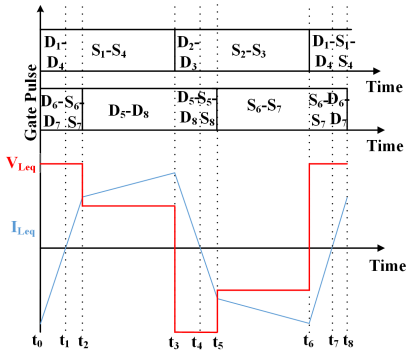


Fig. 3. Voltage and current waveforms of the inductor in forwarding power flow

TABLE I
Switching States of Converter in Buck Mode

| Time duration | Switching States |
|---|---|
| $t_0 < t < t_1$ | $D_1$-$D_4$ and $D_6$-$D_7$ |
| $t_1 < t < t_2$ | $S_1$-$S_4$ and $S_6$-$S_7$ |
| $t_2 < t < t_3$ | $S_1$-$S_4$ and $D_5$-$D_8$ |
| $t_3 < t < t_4$ | $D_2$-$D_3$ and $D_5$-$D_8$ |
| $t_4 < t < t_5$ | $S_2$-$S_3$ and $S_5$-$S_8$ |
| $t_5 < t < t_6$ | $S_2$-$S_3$ and $S_6$-$S_7$ |
| $t_6 < t < t_7$ | $D_1$-$D_4$ and $D_6$-$D_7$ |
| $t_7 < t < t_8$ | $S_1$-$S_4$ and $S_6$-$S_7$ |

### B. Boost operation (Reverse power transfer):

In this mode, the battery starts discharging by supplying energy to the 400 V input DC link which is a boost operation. In this case, generated gate pulses at the HV side VSC lags LV side by an angle $\theta$ and power transfers from secondary to primary side. Switching states of devices are provided in Table-II. The current and voltage across equivalent inductor is shown in Fig. 4, referring gate pulses of both bridges.

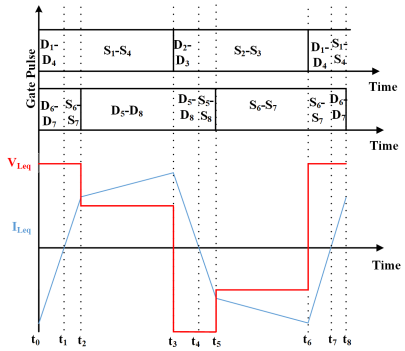


Fig. 4. Voltage and current waveforms of the inductor in reverse power flow

TABLE II
SWITCHING STATES OF CONVERTER IN BUCK MODE

| Time duration | Switching States |
|---|---|
| $t_0 < t < t_1$ | $D_2$-$D_3$ and $S_6$-$S_7$ |
| $t_1 < t < t_2$ | $S_2$-$S_3$ and $D_6$-$D_7$ |
| $t_2 < t < t_3$ | $D_1$-$D_4$ and$D_6$-$D_7$ |
| $t_3 < t < t_4$ | $D_1$-$D_4$ and $S_5$-$S_8$ |
| $t_4 < t < t_5$ | $S_1$-$S_4$ and $D_5$-$D_8$ |
| $t_5 < t < t_6$ | $D_2$-$D_3$ and $D_5$-$D_8$ |
| $t_6 < t < t_7$ | $D_2$-$D_3$ and $S_6$-$S_7$ |
| $t_7 < t < t_8$ | $S_2$-$S_3$ and $D_6$-$D_7$ |

## III. Steady State and Transient Analysis

In this section, the steady state analysis of the DAB converter is performed to establish the relation for high voltage port current. Referring to Fig. 5(a), when the converter is operating in forward power transfer mode, the change in input current during $0 < t \leq \frac{T_s\theta}{2\pi}$ is:

$$\Delta I_{in} = \frac{\theta T_s}{2\pi L}(V_1 + \frac{V_2}{n}) \tag{2}$$

where

$$t_2 = \frac{T_s\theta}{2\pi}$$

The input port current at time instant $t_2$ is :

$$i(t_2) = i(t_0) + \frac{\theta T_s}{2\pi L}(V_1 + \frac{V_2}{n}) \tag{3}$$

Similarly during the time interval $\frac{\theta T_s}{2\pi} < t \leq \frac{T_s}{2}$, the excursion in inductor current and thus the input port current at $t_3$ can be determine as:

$$i(t_3) = i(t_2) + \frac{\theta T_s}{2\pi L}(V_1 + \frac{V_2}{n}) \tag{4}$$

where

$$t_3 = \frac{T_s}{2}$$

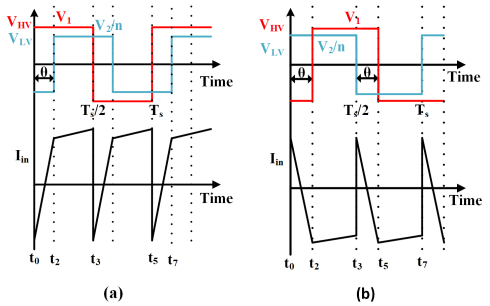


Fig. 5. (a)Voltage and input current waveforms in forward power flow; (b)Voltage and input current waveforms in reverse power flow

### A. Steady State Behaviour of DAB Converter

Considering the inductor as non-dissipative element, under the steady state condition $i(t_3) = -i(t_0)$ and the input current port at time instant $t_0$ is:

$$i(t_0) = \frac{V_2}{n}(1 - \frac{2\theta}{\pi})\frac{T_s}{4L} \tag{5}$$

Using (3) and (5), the input port current at instant $t_2$:

$$i(t_2) = [\frac{V_2}{n} - V_1(1 - \frac{2\theta}{\pi})]\frac{T_s}{4L} \tag{6}$$

Further, behavior of the input port current can be established as follows:

$$i_{La}(t) = i(t_0) + \frac{i(t_1) - i(t_0)}{\frac{\theta T_s}{2\pi}}t \quad ; \quad t_o < t \leq t_2 \tag{7}$$

$$i_{Lb}(t) = i(t_1) + \frac{i(t_2) - i(t_1)}{\frac{T_s}{2}(1 - \frac{\theta}{\pi})}t \quad ; \quad t_2 < t \leq t_3 \tag{8}$$

Thus, the average value of input source (port) current is:

$$i_{inavg} = \int_0^{\frac{\theta T_s}{2\pi}} i_{La}(t)dt + \int_{\frac{\theta T_s}{2\pi}}^{\frac{T_s}{2}} i_{Lb}(t)dt \tag{9}$$

$$i_{inavg} = \frac{V_2}{2n\pi f_s L}\theta(1 - \frac{\theta}{\pi}) \tag{10}$$

### B. Simplified Transient Model

This sub-section proposes the simplified model of DAB converter by relating the input port current and the inductor current. Figs. 5(a) and (b) show that the input port current during half the switching cycle possesses all the information of impact of phase shift, $\theta$ on inductor current. This observation revealed that the port information can be used for analysing the inductor current control using phase shift.

The equivalent circuit of Fig. 6 is used for model development. As shown in the figure, output port is replaced by equivalent load $R_{load}$. Equivalent resistance, $r_{eq}$ is resistance of the effective inductance $L$ (including transformer leakage) and the converter loss referring to the secondary side.During forward power transfer condition, the state space model during interval $0 \leq t < \frac{\theta T_s}{2\pi}$ is:

$$\begin{bmatrix} \dot{i_L} \\ \dot{v_2} \end{bmatrix} = \begin{bmatrix} \frac{-r_{eq}}{L} & \frac{1}{L} \\ \frac{-1}{C} & \frac{1}{RC} \end{bmatrix} \begin{bmatrix} i_L \\ v_2 \end{bmatrix} + \begin{bmatrix} \frac{n}{L} \\ 0 \end{bmatrix} v_1 \tag{11}$$

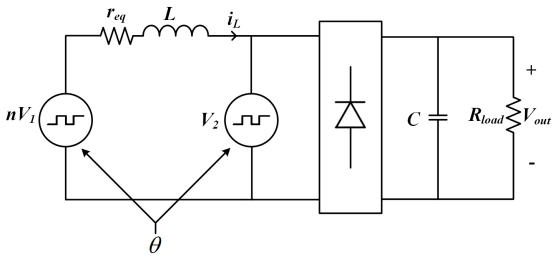

Fig. 6. Equivalent circuit model of DAB converter

Similarly the applicable model during time $\frac{\theta T_s}{2\pi} \leq t < \frac{T_s}{2}$ can be written as:

$$\begin{bmatrix} \dot{i_L} \\ \dot{v_2} \end{bmatrix} = \begin{bmatrix} \frac{-r_{eq}}{L} & \frac{-1}{L} \\ \frac{1}{C} & \frac{-1}{RC} \end{bmatrix} \begin{bmatrix} i_L \\ v_2 \end{bmatrix} + \begin{bmatrix} \frac{n}{L} \\ 0 \end{bmatrix} v_1 \tag{12}$$

Using state space averaging technique for half the switching cycle and relating the phase shift as $d = \frac{\theta}{\pi}$ , a simplified model for a DAB converter, with equivalent circuit shown in Fig. 6, is established as follows:

$$\dot{i_L} = \frac{-r_{eq}}{L} i_L - \frac{(1-2d)}{L} v_2 + \frac{n\ v_1}{L} \tag{13}$$

$$\dot{v_2} = \frac{1-2d}{C} i_L - \frac{1}{RC} v_2 \tag{14}$$

### *C. Control strategy of DAB Converter*

Rearranging (13), the plant transfer function for inductor current is determine as follows:

$$\frac{I_L(s)}{m(s)} = \frac{1}{sL + r_{eq}} \tag{15}$$

where, $m$ relates the actual control variable $d$ as,

$$m = -(1-2d)V_2 + nV_1 \tag{16}$$

Both the ports are supported with capacitors for either reducing the ripple current at load or stresses at the source. In inner current loop, the variation in port voltages are slow enough with respect to the current control bandwidth and thus their average values can be used in feed-forward compensation as follows:

$$d = \frac{m - nV_1}{2V_2} + \frac{1}{2} \tag{17}$$

In DAB bidirectional converter, the objective is to control the power delivery between high and low voltage ports which can be achieved using port current control. Discussion in previous sub-section shows the relation between port current and equivalent inductor current.

The error signal between reference setpoint and output port current is processed through proportionate-integral (PI) compensator to generate the control variable $m$, which can be further passed through feedforward compensation produced in (16). The PI compensator, $G_c = K_p + \frac{K_i}{s}$ can be established for the plant transfer function (15) such that the poorly located plant pole is cancelled by the PI zero, $s = -K_i/K_p$. The time constant of the loop transfer function is adjusted to limit the bandwidth at $f_{Ci} = \frac{1}{10} f_s$. These two conditions leads to the PI values as follows:

$$K_i = \frac{r_L}{\tau}\ ;\quad K_p = \frac{L}{\tau} \tag{18}$$

where, $\tau = \frac{1}{2\pi f_{Ci}}$

The phase shift between two bridges in DAB, $\theta$ is determined from variable $m$ and the delay $d$ which will ensure the zero steady state error. The entire control strategy is shown in Fig. 7.

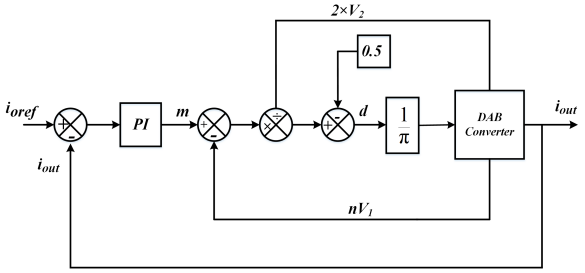

Fig. 7. The current control loop for DAB converter

## IV. Simulation Results

The DAB bidirectional converter is simulated using MATLAB-Simulink to verify the efficacy of proposed simplified model for this converter and to verity the dynamic performance of the close loop control developed using simplified DAB model. In the simulation, the high-frequency transformer is used as the ideal transformer with no losses in core and their equivalent impedance is accounted as series inductance. The system parameters are specified in Table-III. The relevant simulation results for the bidirectional DAB converter with closed-loop control are discussed in this section.

TABLE III
System Parameters Under Study

| Simulation Parameter | Value |
|---|---|
| Input Voltage ($V_{in}$) | 400 V |
| Output Voltage ($V_b$) | 48 V |
| Switching frequency ($f_s$) | 20 kHz |
| Equivalent resistance ($R_{eq}$) | 10 m$\Omega$ |
| Equivalent Inductance ($L_{eq}$) | 46.22 $\mu$H |
| Filter Inductor ($L_f$) | 7.23 nH |
| Filter Capacitor ($C_f$) | 1000 $\mu$F |
| The input capacitor ($C_1$) | 100 $\mu$F |
| Transformation ratio | 3:25 |
| Power rating of Transformer | 10 kVA |

The input port of the bi-directional DC-DC converter is excited with 400 V source. The duty period of both the bridges are 50% (with deadband at each leg) and each bridge operates with 180deg phase angle at between its legs. The phase shift, $\theta$ is the control parameter of the converter provided by the control strategy [Fig. 7]. The bridge converter results into the instantaneous transitions between two levels $\pm$ 400 V. The same effect occur at low voltage side and results into periodic

pulse train of ± 48 V. The frequency of the periodic pulses of both primary and secondary is the same as the switching frequency $f_s$. The phase shift, $\theta$ imparts by the control strategy is introduced between reference legs of the bridges. The results are shown in Fig. 8(a) and (b).

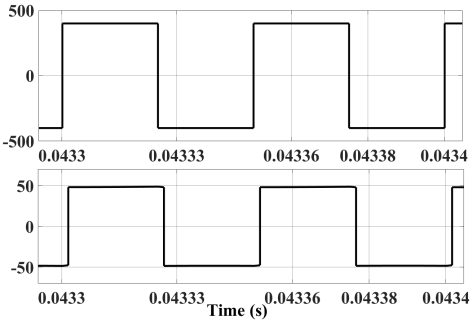


Fig. 8. (a) Primary voltage of transformer in Buck mode; (b) Secondary voltage of Transformer in Buck Mode

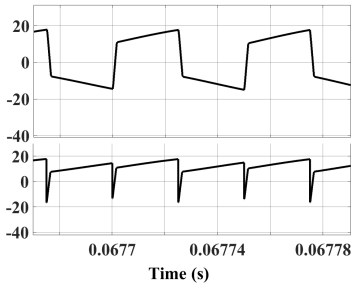


Fig. 9. (a) Inductor current of the converter in Buck mode; (b) Input current of the converter in Buck mode

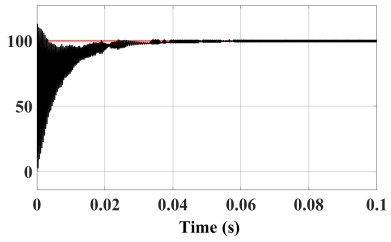


Fig. 10. Output current of the converter in Buck mode

When the positive current reference provided to the control, which is corresponding to the buck mode, the primary voltage leads the secondary voltage as shown in Fig.8, under the steady state condition. The instantaneous inductor current and the port current is shown in Fig. 9. The positive value of actual current at low voltage port shows the power transfer from high voltage port to low voltage port as seen in Fig. 10. It also shows the reference tracking of performance under steady state condition. The actual current follows the reference value of 100A, without steady state error.

The output current has significant ripples which is shown in Fig. 9(b). Unfortunately, the ripple current has large value even at low power transfer and thus filtering at the ports are crucial.

During negative current reference, the phase shift of high voltage side bridge converter lags behind that of low voltage port as shown in Fig. 11. The inductor current and the port current are shown in Fig. 12. For the negative current reference of $I_{oref}$ = -100 Amp, the actual current follows it and achieves zero steady state error as shown in Fig. 13.

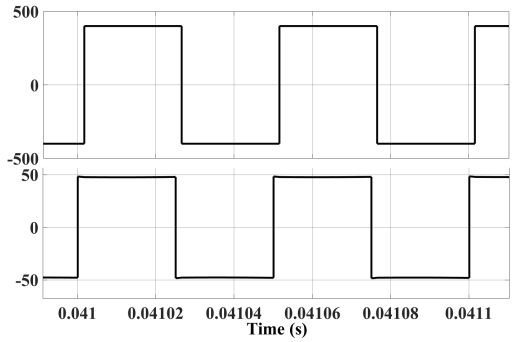


Fig. 11. (a) Primary voltage of transformer in Boost mode; (b) Secondary voltage of Transformer in Boost Mode

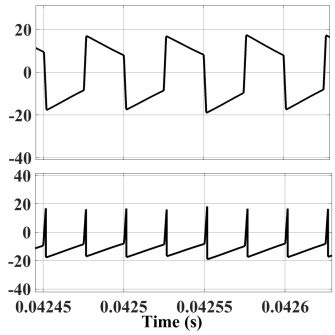


Fig. 12. (a) Inductor current of the converter in Boost mode; (b) Input current of the converter in Boost mode

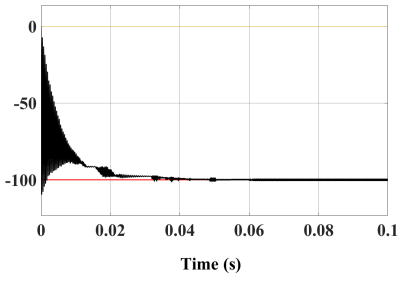


Fig. 13. Output current of the converter in Boost mode

Finally the dynamic performance of close loop control system is evaluated. The Bode plot of plant transfer function and open loop plant transfer function with compensator is shown in Fig. 14. It shows the bandwidth of control close to $\frac{1}{10}^{th}$ of the switching frequency in rad/sec.

The step input reference is provide to the controller to change the current from 80Amp to -40Amp at time instant $t$ =0.05sec. The actual current tracks the reference current in within desired rise time, as shown in Fig. 15. The error response is also shown in Fig. 15. The tracking performance validates the presented model and the formulated control strategy.

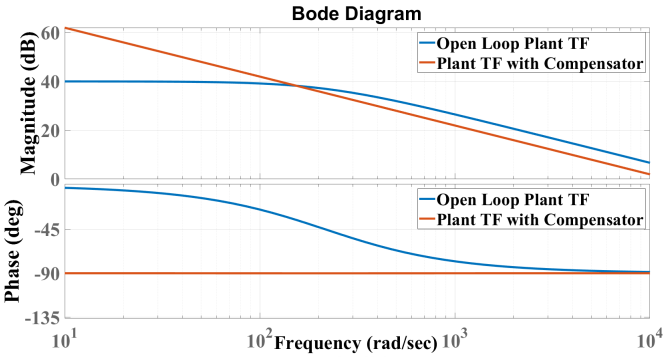

Fig. 14. Bode Plot

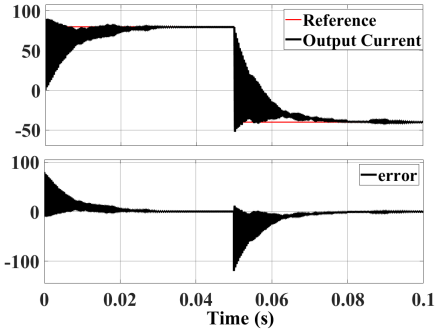

Fig. 15. Output current with step reference

## V. Conclusions

The simplified state-space average model of the Dual Active Bridge power converter and control strategy for output port current are discussed in this paper. This eliminates the complexity in a Fourier based model, if the averaging technique apply over half the cycle of transformer voltage and using input port to AC variable relations. Both steady state and transient analysis are provided to study the behaviour of DAB converter. The analysis is extended to formulate control strategy for close loop control operation using a systematic approach of feedback and feed-forward compensator design. The verification of proposed model using simulation results revealed the effectiveness of model is comparable as that of conventional DAB models. Desired transient response obtained in simulations verified that the simplification in DAB model has not dropped the important attributes relevant to the control operation.

## Acknowledgement

The research work presented in this paper is supported by ”Science and Engineering Research Board (SERB), Department of Science and Technology, Government of India”, under the scheme Start-up Research Grant.

## References

[1] K. Xiangli , S. Li , and K. M. Smedley, “Decoupled PWM Plus Phase-Shift Control for a Dual-Half-Bridge Bidirectional DC–DC Converter,” *IEEE Trans. Power Electron.* , vol. 33, no. 8, pp. 7203-7213, Aug. 2018.

[2] C. Zhang, P. Li, Z. kan, X. Chai, and X. Guo, “Integrated Half-Bridge CLLC Bidirectional Converter for Energy Storage Systems,” *IEEE Trans. Ind. Electron.*, vol. 65, no. 5, pp. 3879–3889, May 2018.

[3] P. Das, B. Laan, S. A. Mousavi, and G. Moschopoulosl, “A nonisolated bidirectional ZVS-PWM active clamped DC-DC converter,” *IEEE Trans. Power Electron.*, vol. 24, no. 2, pp. 553–558, Jan. 2009.

[4] D. Ravi, B. M. Reddy, Shimi S.L., and P. Samuel, “Bidirectional dc to dc Converters: An Overview of Various Topologies, Switching Schemes and Control Techniques,” *International Journal of Engineering and Technology*, vol.7, no. 4.5, pp. 360-365, Sep. 2018.

[5] H. Ardi, A. Ajami, F. Kardan, and S. N. Avilagh, “Analysis and Implementation of a Nonisolated Bidirectional DC-DC Converter with High Voltage Gain,” *IEEE Trans. on Industrial Electron*., vol. 63, no. 8, pp. 4878-4888, Aug. 2016.

[6] Texas Instruments, Modelling, and Optimization of Bidirectional Dual Active Bridge DC-DC Converter Topologies, http://www.ti.com/lit/ug/tidues0/tidues0.pdf.

[7] D. Xu, C. Zhao, and H. Fan,“A PWM plus phase-shift control bidirectional DC-DC converter,” *IEEE Trans. Power Electron.*, vol. 19, no. 3, pp. 666–675, June 2004.

[8] L. Zhu, “A Novel Soft-Commutating Isolated Boost Full-Bridge ZVS-PWM DC-DC Converter for Bidirectional High Power Applications,” *IEEE Trans. Power Electron.*, vol. 21, no. 2, pp. 422–429, March 2006.

[9] H. Li, F. Z. Peng, and J. S. Lawler, “A Natural ZVS Medium-Power Bidirectional DC-DC Converter with Minimum Number of Devices,” *IEEE Trans. on Industry Applications*, vol. 39, no. 2, pp. 525-535, Mar./Apr. 2003.

[10] O. C. Onar, J. Kobayashi, Dylan C. Erb, and Alireza Khalighl, “A Bidirectional High-Power-Quality Grid Interface with a Novel Bidirectional Noninverted Buck-Boost Converter for PHEVs,” *IEEE Trans. on Vehicular Tech.*, vol. 61, no. 5, pp. 2018-2032, June 2012.

[11] H. Qin, and J. W. Kimball, “Generalized Average Modeling of Dual Active Bridge DC-DC Converter,” *IEEE Trans. Power Electron.* , vol.27, no. 8, April 2012.

[12] S. Inoue, and H. Akagi,“A Bidirectional DC–DC Converter for an Energy Storage System With Galvanic Isolation,” *IEEE Trans. Power Electron.*, vol. 22, no. 6, pp. 2299–2307, Nov. 2007.

[13] Amirnaser Yazdani, and Reza Iravani, Voltage-sourced converters in power systems modeling, control, and applications, *IEEE Press John Wiley*, 2010.

[14] VSS Kumar, and D Thukaram,“State estimation in power systems using linear model infinity norm-based trust region approach,” *IET Gener. Transm. Distrib* , vol. 7, Iss. 5, pp. 500-510, 2013.